RADIATION RESEARCH **166**, 802–809 (2006)
0033-7587/06 $15.00

Power Saturation of ESR Signal in Ammonium Tartrate Exposed to ^{60}Co γ-Ray Photons, Electrons and Protons

Maurizio Marrale,[a,c,1] Maria Brai,[a,c] Alessandro Triolo,[a] Antonio Bartolotta[b,c] and Maria Cristina D'Oca[b]

[a] *Dipartimento di Fisica e Tecnologie Relative, Università di Palermo, Viale delle Scienze, Edificio 18, 90128 Palermo, Italy;* [b] *Dipartimento Farmacochimico Tossicologico e Biologico, Università di Palermo, Via Archirafi 32, 90123 Palermo, Italy; and* [c] *Unità CNISM, Palermo and Gruppo V, Sezione INFN, Catania*

Marrale, M., Brai, M., Triolo, A., Bartolotta, A. and D'Oca, M. C. Power Saturation of ESR Signal in Ammonium Tartrate Exposed to ^{60}Co γ-Ray Photons, Electrons and Protons. ***Radiat. Res.*** **166, 802–809 (2006).**

In this paper we present an investigation of the electron spin resonance (ESR) line shape of ammonium tartrate (AT) dosimeters exposed to radiation with different linear energy transfer (LET). We exposed our dosimeters to γ-ray photons (^{60}Co), 7 MeV and 14 MeV initial energy electrons, and 19.3 MeV initial energy protons. The differences in the power saturation behavior of ESR spectra of AT irradiated with photons, electrons and protons could be correlated to the effective LET of the radiation beams. We analyzed the behavior of peak-to-peak amplitude as a function of microwave power, and we developed a fitting procedure that permits us to obtain the dependence of the homogeneity parameter of the line shape on the LET of the radiation using the Castner saturation theory. This simple procedure allows us to distinguish the LET of the radiation beam.

INTRODUCTION

Ionizing radiation dosimetry based on measurements of free radicals produced in several materials using electron spin resonance (ESR) spectroscopy is a well-established and extensively studied method. Unlike other methods, for instance thermoluminescence, the EPR technique permanently saves the information after exposure to radiation, allowing repeated readings for multiple and different acquisitions of the signal of the free radicals in the dosimeter. This property is a great advantage for postelaboration and analyses of several parameters of the spectrum.

In 1962 (*1*) the first dosimetric application of the ESR technique was realized using powder samples of α-alanine. These experiments led to the use of alanine as a dosimetric material. Regulla and Deffner (*2*) developed solid-state alanine pellets with paraffin as a binding material to be used as dosimeters. Alanine dosimeters today are ordinarily produced in the shape of capsules, films or cables for applications in the fields of industrial irradiation, sterilization, etc. The remarkable dosimetric features of alanine are that the ESR response is linear over a large dose range (10–10^4 Gy), its energy dependence is similar to that of standard biological tissue, and the free radicals induced after irradiation are highly stable under standard storage conditions. Nette *et al.* (*3*) showed the possibility of measuring absorbed dose at 2 Gy with a precision of ±2% by means of alanine pellets. The relative sensitivity of alanine does not allow accurate measurements of doses lower than 1 Gy. This prevents wide applications of alanine dosimeters in radiotherapy, where the dose measurements must be performed with high sensitivity (and lowest detectable dose less than 1 Gy) and with an uncertainty of less than 3%.

Nevertheless, there are great advantages in the application of ESR to radiotherapeutic dosimetry, since ESR dosimetry is not affected by read-out and thus the information is preserved. In fact, a single dosimeter can be used to follow the radiotherapeutic treatment, often constituted by dose fractionation, and to furnish an indication of the integrated absorbed dose (*4*).

There is interest in finding new materials for ESR dosimetry of high sensitivity that are capable of detecting doses smaller than 1 Gy. In the last 5 years, studies were conducted in various laboratories to find such new materials (*5–7*) with a high efficiency of radiation energy transfer, sharp spectral lines and time stability of the radicals at room temperature. Among the different materials tested, ammonium tartrate (AT) is one of the most studied (*4, 8–10*). This substance has a signal-to-noise ratio higher than that of alanine (approximately double in its standard composition and approximately triple if the hydrogen atoms are replaced with deuterium).

The response behavior of ammonium tartrate dosimeters to clinical photon, electron and proton beams was studied previously by our group (*9, 11*). Our results suggested AT as a good candidate for application in radiotherapy as well as for dosimetry of high-LET radiation.

When a biological tissue is irradiated, detailed informa-

[1] Address for correspondence: Dipartimento di Fisica e Tecnologie Relative, Università di Palermo, Viale delle Scienze, Edificio 18, 90128 Palermo, Italy; e-mail address: marrale@difter.unipa.it.

tion on the radiation quality is very important from a radiobiological point of view, because biological effects are strongly related to the linear energy transfer (LET) of the radiation beam as well as to dose. A dosimetric technique that can give information on dose and on radiation quality is therefore preferable, particularly for mixed-field irradiations. The techniques usually used to distinguish the LET of the radiation beam are tissue-equivalent proportional counters, chemically etched track detectors (*12*), thermoluminescence dosimeters through the high-temperature ratio method, and other methods (*13, 14*). The aim of the work described here was to study the variations in the shape and the power saturation characteristics of the ESR signal in ammonium tartrate dosimeters after irradiation with beams of different quality to investigate the possibility of using ESR dosimetry to discriminate the LET of the radiation beam.

The analysis of power saturation was performed using the first derivative of the ESR absorption signal. The shortcut of analyzing ESR spectra using the peak-to-peak method instead of the integral of the ESR absorption is outlined. Finally, it is shown that some parameters of the power saturation fitting curve can be used for the determination of radiation quality. Since no dependence of the line shape and line width on dose was observed, we used doses that produced adequate S/N ratios. The dosimetric properties previously found by our group for different radiation beams are summarized briefly for completeness.

MATERIALS AND METHODS

Solid-State Dosimeters

A homogeneous blend of ammonium tartrate (Carlo Erba, Italy), polyethylene (Polysciences, molecular weight = 700) and magnesium stearate (Carlo Erba) (94, 5 and 1% by weight, respectively) was prepared. The three compounds were mixed in a powder blender (Laboratori MAG, Italy), and the blend was stored in a controlled environment until used. Solid-state cylindrical pellets were obtained by using small stainless steel pistons to press 24 mg of the blend previously inserted into each housing of a stainless steel die; a pressure of about 6×10^6 Pa was applied to obtain pellets with an expected thickness of 1 mm and diameter of 4.8 mm. The pellets were subjected to a thermal cycle of 20 min at 130°C and 15 min at 85°C to improve their mechanical properties (*9*).

The samples used in this experiment belong to the same batch of 500 dosimeters used previously to investigate dosimetric properties with photon, electron and proton beams as described in the section on *Dosimetric Properties,* and they have been stored for more than 3 years at room temperature and standard humidity.

The mass and size of 100 ammonium tartrate pellets, randomly chosen from the batch, were measured: diameter 4.80 mm, thickness 0.96 mm, mass 22.2 mg. The mean mass density of the dosimeters was therefore 1.28 g cm^{-3}. The ratio of mass weighted atomic number to atomic weight was 0.535.

Irradiations

Dosimeters were irradiated using four different beams with LET: ^{60}Co γ-ray photons, 7 and 14 MeV initial energy electrons, and 19.3 MeV initial energy protons.

Irradiations with ^{60}Co γ-ray photons, 1.25 MeV mean energy and equivalent LET in ammonium tartrate of ~0.3 keV μm^{-1}, were carried out under conditions of electronic equilibrium with the IGS-3 irradiator in the Dipartimento di Ingegneria Nucleare, Università di Palermo. The dose rate was 2.6 kGy/h as measured with Fricke dosimetry. The dosimeters were irradiated with three different doses, 0.1, 1 and 5 kGy, with an overall uncertainty of 3%.

Irradiations with electron beams were performed inside a solid water phantom ($15 \times 15 \times 4$ cm^3) using a linear accelerator employed for radiotherapy treatments at Centro Oncologico 'M. Ascoli', ARNAS, Palermo. The initial electron energies were 7 MeV and 14 MeV, with effective LET in ammonium tartrate of 0.25 keV μm^{-1} and 0.26 keV μm^{-1}, respectively. The doses were measured with a Markus chamber with 2% uncertainty. Since this facility is used for radiotherapy, we could perform irradiations only at 0.1 kGy for both initial energy values.

Proton irradiations were performed at the Tandem accelerator facility of the Istituto Nazionale di Fisica Nucleare (INFN-LNS) at Catania. This accelerator was used to produce proton beams with 22 MeV source energy and with a maximum current of 75 mA. The beam goes through a 75-μm-thick aluminum window, a Markus chamber used for monitoring the proton fluence stability, and 60.2 cm of air before reaching the surface of the phantom used for dosimeter irradiation. The dosimeters were located on the phantom surface. The proton beam energy at the phantom surface was determined to be 19.3 MeV, with an effective LET in ammonium tartrate of 3.46 keV μm^{-1}; the effective transverse section area of the beam was circular, with a diameter of 2.5 cm on the phantom surface. The absorbed dose rate has been computed through a numerical integration of the following equation on the dosimeter thickness:

$$\left(\frac{dD}{dt}\right)_p = 1.602 \times 10^{-10}\left\{\frac{S[E(x)]}{\rho}\right\}\frac{I}{A_S e},$$

where A_S is the effective transversal section area of the beam in cm^2, $S(E(x))/\rho$ is the mass stopping power in the dosimeter at the depth x in MeV cm^2/g, I is the beam current measured with a Faraday cup, and e is 1.602×10^{-19} C. The absorbed dose rate was 0.25 kGy/min. Three nominal doses were obtained: 0.1, 1 and 5 kGy.

ESR Measurements

The ESR spectra were always recorded at room temperature with a Bruker ECS106 spectrometer equipped with a TE_{102} rectangular cavity operating at approximately 9.7 GHz. The tartrate pellets were reproducibly positioned inside the cavity, in the location of maximum signal intensity, by means of a quartz vial and quartz spacers.

The following parameters, carefully chosen to preserve the line shape and to avoid any distortion due to a large modulation amplitude compared to the line width, were set for the acquisition of the spectra:

1. field center, 349.0 mT;
2. field sweep, 10.0 mT;
3. modulation amplitude, 0.10 mT;
4. modulation frequency, 50 kHz;
5. time constant, 1311 ms;
6. sweep time, 168 s.

The receiver gain was set differently for different dose values and consequently for different spin concentrations in the dosimeters. For the dosimeters irradiated with 0.1 kGy, the lowest dose used, we accumulated two scans to increase the signal-to-noise ratio.

Since it is known that the ESR signal of AT dosimeters changes during the first few days after irradiation (*8, 9*) and remains almost stable afterward, we always performed the ESR measurements approximately 170 h after irradiation; 23 spectra, with power between 1 μW and 25 mW from maximum attenuation of 53 dB to 9 dB with 2-dB steps, were recorded for every dose value and for every type of beam.

Dosimetric Properties

The main dosimetric properties of the batch of dosimeters used in these studies are summarized here.

TABLE 1
Relative Effectiveness (RE) of Ammonium Tartrate for Different Quality Beams with Respect to ^{60}Co γ Rays

Radiation beam	RE
^{60}Co gamma rays	1
X rays, 85 kV[a]	0.80 ± 0.03
X rays, 18 MV[a]	1.00 ± 0.03
Electrons, 9 MeV[a]	1.01 ± 0.03
Electrons, 21 MeV[a]	1.02 ± 0.02
Protons, 13.2 MeV[b]	0.89 ± 0.03
Protons, 19.1 MeV[b]	0.95 ± 0.03
Protons, 58.6 MeV[b]	1.00 ± 0.03

[a] Bartolotta *et al.* (*9*).
[b] Bartolotta *et al.* (*11*).

For dosimetric purposes the ESR spectra were recorded at a microwave power of 1.59 mW and modulation amplitude of 0.88 mT to maximize the signal-to-noise (S/N) ratio. Using this experimental setup, the value of the S/N for a dosimeter irradiated with ^{60}Co γ-ray photons at a dose of 30 Gy was 37.5; this value is 2.5 times the corresponding value measured in alanine solid-state dosimeters with a mass equal to that of the ammonium tartrate pellets and irradiated with the same procedure (*9*).

The ESR signal amplitude of ammonium tartrate dosimeters was studied as a function of dose by irradiating 11 groups of three dosimeters at 11 calibration doses with the ^{60}Co γ rays in the 0.5–50-Gy range. The lowest detectable dose, defined as the dose that produces an ESR signal in the irradiated dosimeter equal to the mean value of the background in unirradiated dosimeters plus three standard deviations, is 0.5 Gy.

A parameter that must be considered in the response analysis is the relative effectiveness (RE). The relative effectiveness is defined as the ratio of the ESR signal amplitude of dosimeters irradiated with a particular beam to the amplitude of that of one of the dosimeters irradiated at the same dose with ^{60}Co γ-ray photons. The values of the relative effectiveness for the photon, electron and proton beams are reported in Table 1.

No significant dependence of the response on beam quality was evident for photon beams with energy higher than ^{60}Co γ rays or for high-energy electron beams, whereas dose underestimation was observed for low-energy X-ray beams. A slight decrease in RE was found with decreasing proton energy up to about 10% at the mean energy of 13.2 MeV. These results suggest the necessity of carrying out line shape and power saturation analyses on spectra of the irradiated dosimeters to determine the dependence of saturation parameters on radiation quality.

Microwave Power Saturation Analysis

According to the literature (*15, 16*), the expression of the absorption curve of an inhomogeneously broadened line, i.e. a convolution of a Lorentzian function with a Gaussian function, is as follows (Castner Function):

$$A(B) \propto \frac{B_1}{\Delta B_G \Delta B_L} \int_0^\infty \frac{B' \exp\left[-\left(\frac{B' - B_0}{\Delta B_G}\right)^2\right] dB'}{1 + \left(\frac{B - B'}{\Delta B_L}\right)^2 + \gamma^2 B_1^2 T_1 T_2}, \quad (1)$$

where T_1 and T_2 are, respectively, the spin-lattice and spin-spin relaxation times; ΔB_G is the width of the Gaussian distribution of the inhomogeneous broadening, ΔB_L represents the width of the Lorentzian single spin packet and is inversely proportional to T_2 ($\Delta B_L \approx 1/(\gamma T_2)$); B_0 represents the central field of the Gaussian distribution; B_1 is the intensity of the microwave oscillating magnetic field; γ is the gyromagnetic ratio for the system under investigation; B' is the running variable, i.e. a magnetic field.

The maximum amplitude of the absorption signal is (*16*)

$$V_R \propto \frac{\frac{x}{x_0}}{\sqrt{1 + \left(\frac{x}{x_0}\right)^2}} \exp\left[a^2 \left(\frac{x}{x_0}\right)^2\right] \frac{\mathrm{Erfc}\left[a\sqrt{1 + \left(\frac{x}{x_0}\right)^2}\right]}{\mathrm{Erfc}[a]}, \quad (2)$$

where $a = \Delta B_L / \Delta B_G$ is a parameter that measures the degree of inhomogeneity of line broadening; x is the microwave power square root ($\sqrt{P} \propto B_1$); $x_0 \propto 1/\sqrt{\gamma^2 T_1 T_2}$ is the saturation parameter defined as $(x/x_0)^2 = \gamma^2 B_1^2 T_1 T_2$, and *Erfc* is the complementary error function equal to

$$1 - \frac{2}{\sqrt{\pi}} \int_0^x e^{-t^2}\, dt.$$

It was shown previously (*17*) that Eq. (1), which represents the convolution of a Lorentzian spin packet in a Gaussian envelope, can be arranged into the following shape function, neglecting any factor that represents the transition probability of the line:

$$A(B) \propto \frac{a}{\Delta B_L^2} \frac{\sqrt{P}}{t} u(a \cdot r,\, a \cdot t), \quad (3)$$

where

$$r = \frac{B - B_0}{\Delta B_L}, \qquad t = \sqrt{1 + \gamma^2 B_1^2 T_1 T_2},$$

and $u(a \cdot r, a \cdot t)$ is the real part of the complex function

$$w(z) = \exp(-z^2)\mathrm{erfc}(-iz) \quad \text{and} \quad z = i \cdot a \cdot t + a \cdot r. \quad (4)$$

Equation (3), evaluated for $r = 0$ ($B = B_0$), is related to Eq. (2).

With this equation, it is possible to understand that a well-defined relationship exists between the trend of maximum of the absorption curve, the microwave power and the a value. In the limit for a that tends to 0 (for completely inhomogeneous broadening), the V_R value tends to a constant value with increasing power. In the limit for a that tends to infinity (for completely homogeneous broadening), V_R increases linearly with power, reaches a maximum and for power values very much larger than $1/\sqrt{\gamma^2 T_1 T_2}$ tends to zero as x^{-1}.

The goal of our power saturation study was to obtain some parameters that would allow one to distinguish the quality of the radiation beams.

Therefore, we tried to fit the maximum of the ESR absorption curve, obtained by integrating the signal, as a function of $\sqrt{P}$. This procedure experienced problems from baseline drift in spectra, especially for the dosimeters irradiated with 0.1 kGy. The low frequency distortion of the baseline varies from sample to sample and is not readily removed by simple background subtraction (*18–20*); moreover, the numerical subtraction could introduce artifacts in the experimental data.

Therefore, we decided to carry out the analysis using the peak-to-peak amplitude of the measured ESR first derivative as a function of microwave power. To perform this analysis, we used the first derivative of Eq. (3) with respect to the magnetic field B:

$$F_1(B) = \frac{dA(B)}{dB} \propto -\frac{2a^3}{\Delta B_L^4} \sqrt{\frac{x_0^2 x^2}{x_0^2 + x^2}}\, \mathrm{Re}\left\{\left(\frac{B - B_0}{\Delta B_L} + i\sqrt{1 + \frac{x^2}{x_0^2}}\right) \times \exp\left[-a^2\left(\frac{B - B_0}{\Delta B_L} + i\sqrt{\frac{x^2}{x_0^2 + x^2}}\right)^2\right] \times \mathrm{Erfc}\left[a\left(-i\frac{B - B_0}{\Delta B_L} + \sqrt{1 + \frac{x^2}{x_0^2}}\right)\right]\right\}, \quad (5)$$

where Re{. . . } is the real part of the complex function in brackets; we studied the trend of the peak-to-peak amplitude of this function [which is two times its maximum value, since $F_1(B)$ is antisymmetrical with respect to B_0] with increasing power. To obtain this trend, it is necessary

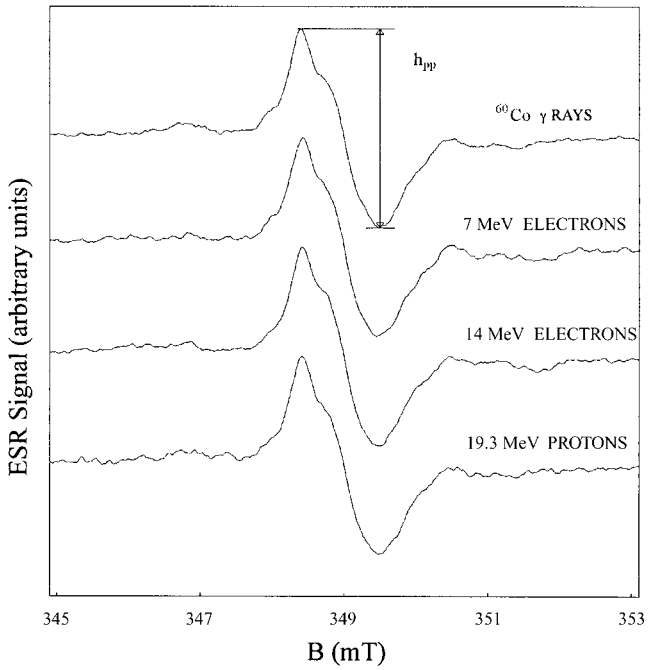

FIG. 1. ESR spectra of ammonium tartrate dosimeters irradiated with (0.1 kGy) ^{60}Co γ-ray photons, 7 and 14 MeV electrons, and 19.3 MeV protons. The peak-to-peak amplitude h_{pp} is also shown.

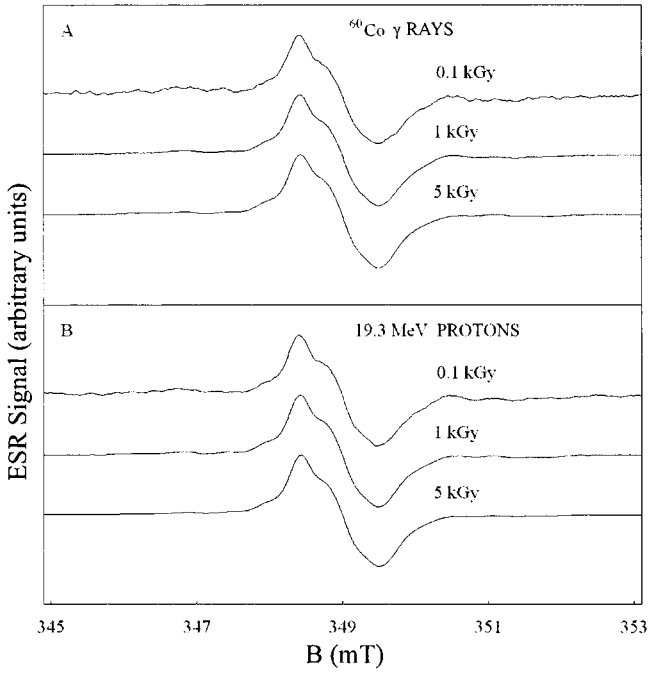

FIG. 2. ESR spectra of ammonium tartrate dosimeters irradiated with ^{60}Co γ-ray photons (panel A) and 19.3 MeV protons (panel B) at 0.1, 1 and 5 kGy.

to find the zeros of the first derivative $F_1(B)$ of Eq. (5) [i.e. the zeros of the second derivative of Eq. (3)]. The equation obtained by setting $F_2(B) = dF_1/dB = d^2A/dB^2$ to zero is transcendental because of the presence of the complementary error function; i.e., an analytical solution of this equation does not exist. Therefore, one of the zeros of $F_2(B)$; i.e., the B value where $F_1(B)$ reaches its maximum values, F_{1MAX}, was determined numerically. The peak-to-peak amplitude $\Delta F = 2\ F_{1MAX}$ was calculated for each of the microwave power values used in our experiments. ΔF depends on the physical parameters T_1, T_2 and $\Delta B_L/\Delta B_G$; for each dose value and for each radiation beam used in our experiments, a numerical iterative fit of the experimental peak-to-peak height of the recorded ESR spectra was carried out using ΔF. The parameters $x_0^2 \times T_2$ ($\propto 1/T_1$), T_2, a and a scale factor A were optimized to minimize the χ^2 value. The best estimates of $x_0^2 \times T_2$, T_2, a and A were obtained for each dose and each beam, adopting the following procedure. We considered, for a specific dose value and for a specific beam type, the trend of the experimental peak-to-peak amplitudes of ESR signal. For each microwave power value used in these experiments, we found numerically the maximum value of Eq. (5) using some trial values for a, $x_0^2 \times T_2$, T_2 and A. By comparison of the trend of the experimental data with the trend of values found numerically, we obtained the ranges wherein the parameters a, $x_0^2 \times T_2$, T_2 and A can vary. The iterative numerical procedure consists of the following steps:

1. calculation of the values of the maximum of expression (5) as a function of power, using values of each parameter equally spaced inside its own range;
2. choice of the set of the parameters that minimize the χ^2 value;
3. reiteration of steps (1) and (2) by restricting the ranges each time until the step amplitude for each of the four parameters was smaller than 0.1%.

We obtained an estimate of the uncertainty of these parameters in the analysis described above by taking into consideration the experimental data ±1 SD.

In our study we analyzed the trend of the peak-to-peak amplitude of ESR signal as discussed in the Results and Discussion. More than one EPR line contributes to the peak-to-peak amplitude of the AT ESR signal. The various radiation beams determine different power saturation behaviors for all lines that contribute to the peak-to-peak amplitude, whose trend is influenced by all these lines. It is necessary to emphasize that the analysis we have reported above refers to a single line spectrum. In this case, for the AT signal, we use this method because it permits us to extract parameters that are sensitive to LET. The parameters we obtained from the numerical fit can be considered as a value averaged over all the radical species produced by the radiation.

In the following analysis, the peak-to-peak amplitudes of the ESR signals of the dosimeters exposed to radiations of different quality at different doses are compared.

RESULTS AND DISCUSSION

Figure 1 shows the ESR spectra of dosimeters irradiated with ^{60}Co γ-ray photons, 7 and 14 MeV electrons, and 19.3 MeV protons at a dose of 0.1 kGy.

The line shape of the spectra is apparently independent of beam quality even though the ESR spectra are composed of more than one line. A detailed analysis of the existing radical species is beyond the scope of the work. However, any difference in the radical concentrations attributable to beam quality does not invalidate our results, which emphasize the dependence of saturation behavior of the ESR signal on the beam quality.

Figure 2 shows the spectra of dosimeters irradiated with ^{60}Co γ-ray photons (panel A) and with protons (panel B) at three doses (0.1, 1 and 5 kGy). No dependence of line shape on dose is evident.

Figure 3 shows two spectra, recorded at low and high microwave power, of ammonium tartrate dosimeters irradiated with ^{60}Co γ-ray photons (panel A) and with protons

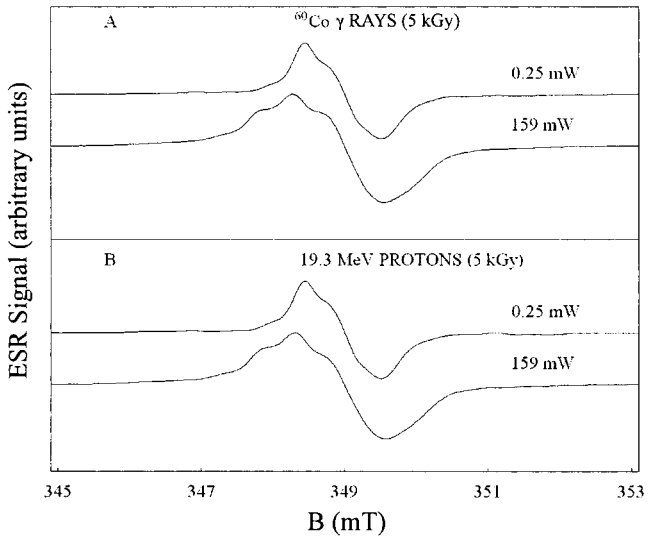

FIG. 3. ESR spectra of ammonium tartrate dosimeters irradiated with 5 kGy ^{60}Co γ-ray photons (panel A) and 19.3 MeV protons (panel B), recorded at 0.25 mW (linear region) and 159 mW (saturation region).

(panel B). Since the central line is always well resolved, we can focus our study on the central line, unlike the case of alanine spectra (*21*), for which the ratio between the intensity of satellite lines and the intensity of the central line was analyzed as a function of microwave power.

Figures 4, 5 and 6 show the peak-to-peak amplitude (h_{pp}) as a function of the square root of microwave power ($\sqrt{P}$) for all the radiation beams and doses used in this work.

For microwave power values smaller than 0.25 mW, the line shape does not change and h_{pp} increases proportionally with the square root of the power.

For microwave power values greater than 0.25 mW, because of power saturation, the line shape is distorted with respect to the initial shape, and h_{pp} reaches its maximum and decreases afterward. Figures 4, 5 and 6 also show the best-fitting curves obtained through the numerical iterative procedure described above.

In particular, Fig. 4 shows the experimental values of the

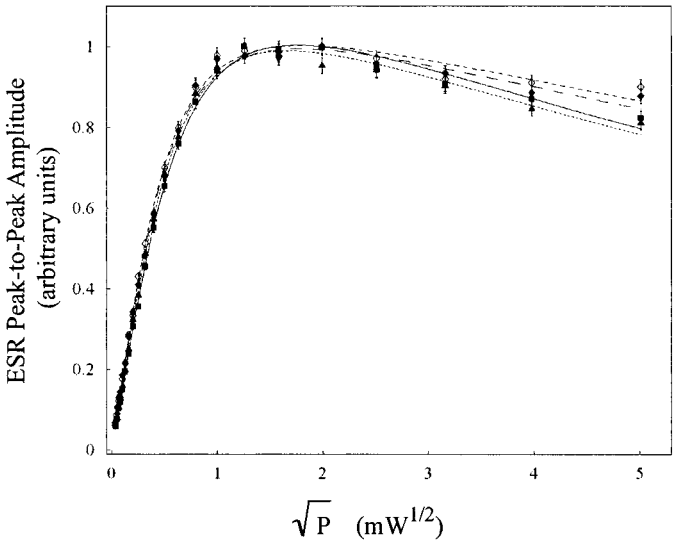

FIG. 4. Experimental values of power saturation study for the ammonium tartrate radicals induced by 0.1 kGy of ^{60}Co γ-ray photons (▲), 7 MeV electrons (♦), 14 MeV electrons (◇) and 19.3 MeV protons (■). The signal amplitude for each radiation beam was divided by its own maximum value. The error bars correspond to ±1 SD. The best-fitting curves are also shown: ^{60}Co photons (· · · · · · · · ·), 7 MeV electrons (— —), 14 MeV electrons (– – –), and 19.3 MeV protons (———).

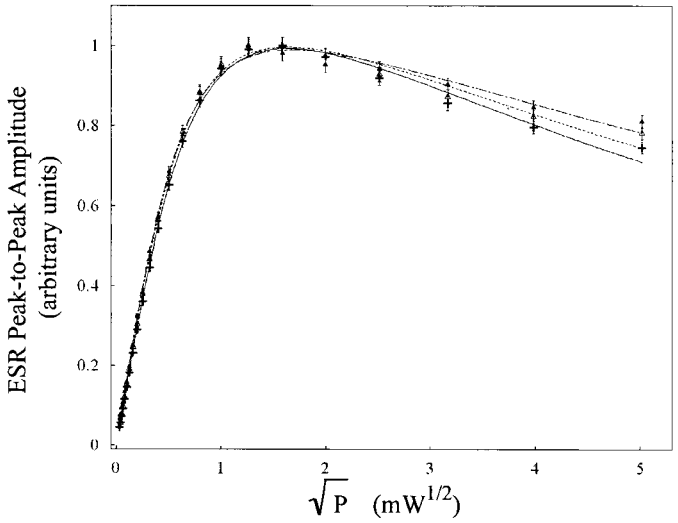

FIG. 5. Experimental values from the power saturation study for the ammonium tartrate radicals induced by 0.1 kGy (▲), 1 kGy (△) and 5 kGy (+) of ^{60}Co γ-ray photons. The signal amplitude for each dose value was divided by its own maximum value. The error bars correspond to ±1 SD. The best-fitting curves are also shown: 0.1 kGy (— · —), 1 kGy (· · · · · · · · ·) and 5 kGy (———).

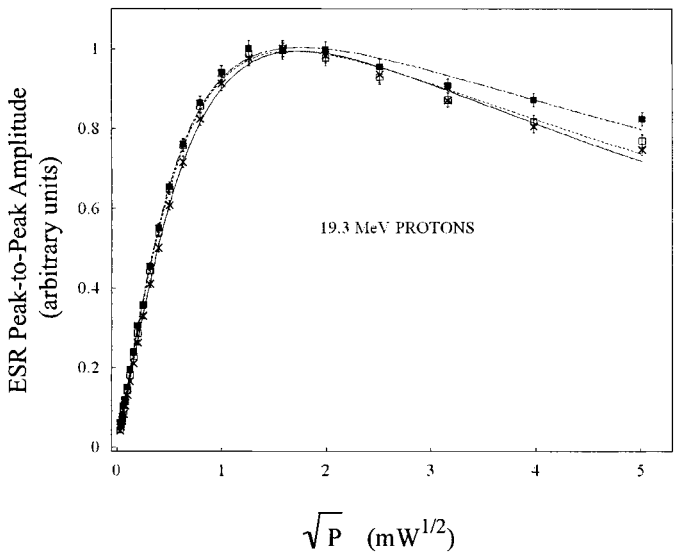

FIG. 6. Experimental values from the power saturation study for the ammonium tartrate radicals induced by 0.1 kGy (■), 1 kGy (□) and 5 kGy (×) of 19.3 MeV protons. The signal amplitude for each dose value was divided by its own maximum value. The error bars correspond to ±1 SD. The best-fitting curves are also shown: 0.1 kGy (— · —), 1 kGy (· · · · · · · · ·), and 5 kGy (———).

TABLE 2
Parameters Obtained by Numerical Fit of Data of Figure 4 at a Dose of 0.1 kGy

Radiation beam	Energy (MeV)	LET (keV μm^{-1})	$a/10^{-2}$	$x_0^2 \times T_2$ (mW μs)	T_2 (μs)	$x_0/10^{-1}$ ($mW^{1/2}$)	Slope of linear fit up to 0.25 mW
γ-ray photons	1.25 (^{60}Co)	~0.3 (equivalent LET)	4.0 ± 0.4	1.94 ± 0.11	3.8 ± 0.2	7.1 ± 0.3	1.59 ± 0.05
Electrons	7	0.25	2.6 ± 0.3	2.07 ± 0.13	4.8 ± 0.3	6.5 ± 0.3	1.69 ± 0.06
Electrons	14	0.26	2.3 ± 0.3	2.07 ± 0.14	5.2 ± 0.3	6.3 ± 0.3	1.71 ± 0.07
Protons	19.3	3.46	4.5 ± 0.5	2.00 ± 0.11	3.3 ± 0.2	7.8 ± 0.3	1.49 ± 0.04

peak-to-peak amplitude as a function of the square root of microwave power at 0.1 kGy for four radiation beams.

In Table 2, we report the values of parameters a, T_2, $x_0^2 \times T_2$ of numerical fitting of these saturation curves. The values of the parameter T_2, obtained through this microwave power saturation analysis are just estimates of the real transversal relaxation time. The x_0 values, related to maximum position, were also calculated.

In the last column of Table 2 the slope of the linear fit up to 0.25 mW is reported. This slope is related to the a, T_2 and x_0 parameters. The analysis of ΔF (introduced in section *Microwave Power Saturation Analysis*) as a function of $\sqrt{P}$ in the linear range shows that this slope decreases when either a and/or x_0 increase and/or T_2 decreases. Consequently, any change in the slope of ΔF as a function of $\sqrt{P}$ is indicative of a variation of at least one parameter.

The values (about 10^{-2}) of the parameter a (which gives information on the line homogeneity) point out that the line is prevalently inhomogeneously broadened.

The a parameter for dosimeters exposed to high-LET charged particles is significantly greater than for dosimeters exposed to low-LET charged particles; i.e., the homogeneity of all lines decreases with decreasing LET. This involves a more homogeneous broadening due to a more intense dipolar interaction between like spins. The values of the relaxation time T_2 increase with decreasing LET, whereas the values of the parameter $x_0^2 \times T_2$ do not vary significantly. Moreover, the maximum value of the trend is reached for the protons at greater microwave power than for the γ-ray photons. The slope of the linear fit up to 0.25 mW confirms this finding.

Figures 5 and 6 and Table 3 report the analyses for photon and proton irradiations at different doses.

The value of a increases with dose, indicating that the spin system tends to more homogeneously broadened lines. This indicates that the population of like spins grows with increasing dose.

For all doses, the saturation parameter x_0 and the homogeneity broadening parameter a are greater for dosimeters irradiated with protons than for those irradiated with photons.

In conclusion, four main results were observed:

1. The saturation parameter value x_0 is greater (and the relaxation time T_2 is smaller) in dosimeters irradiated with protons than in dosimeters exposed to electrons and to γ-ray photons.
2. The trend of the dosimeters irradiated with electrons is much more inhomogeneous than that of the dosimeters irradiated with protons.
3. The homogeneity parameter a increases with dose.
4. The parameter $x_0^2 \times T_2$ is approximately independent of beam quality and of radiation dose.

The results reported for item 1 indicate that ammonium tartrate exposed to high-LET radiation (protons of 19.3 MeV initial energy) saturates at greater microwave power than AT exposed to low-LET beams. This is in agreement with the experimental results reported in the literature for alanine (*21*). To explain this result, we have considered the dependence of x_0 on the radical concentrations. It is known that the higher ionization density produced by protons causes a notable increase in the local free radical concentrations.

TABLE 3
Parameters Obtained by Numerical Fit for Three Doses of ^{60}Co γ-Ray Photons and 19.3 MeV Protons

Parameter	Radiation	0.1 kGy	1 kGy	5 kGy
$a/10^{-2}$	1.25 MeV photons	4.0 ± 0.4	5.3 ± 0.5	7.1 ± 0.6
	19.3 MeV protons	4.5 ± 0.5	6.4 ± 0.6	8.8 ± 0.7
$x_0^2 \times T_2$ (mW μs)	1.25 MeV photons	1.94 ± 0.11	2.16 ± 0.11	1.87 ± 0.07
	19.3 MeV protons	2.00 ± 0.11	2.06 ± 0.10	1.95 ± 0.08
T_2 (μs)	1.25 MeV photons	3.8 ± 0.2	3.68 ± 0.17	2.64 ± 0.09
	19.3 MeV protons	3.3 ± 0.2	2.95 ± 0.13	2.09 ± 0.07
$x_0/10^{-1}$ ($mW^{1/2}$)	1.25 MeV photons	7.1 ± 0.3	7.7 ± 0.3	8.4 ± 0.3
	19.3 MeV protons	7.8 ± 0.3	8.4 ± 0.3	9.6 ± 0.3
Slope of linear fit up to 0.25 mW	1.25 MeV photons	1.59 ± 0.05	1.48 ± 0.02	1.42 ± 0.02
	19.3 MeV protons	1.49 ± 0.04	1.41 ± 0.01	1.30 ± 0.01

The spatial distribution of the absorbed dose around the tracks of the heavy charged particles may reflect the spatial distribution of the final concentration of stabilized free radicals. Consequently, as reported in the literature (*21, 22*), an increase of dipolar spin-spin interaction among radicals clustered along the tracks and a reduction of the relaxation time T_2 are observed. Since x_0 is inversely proportional to the square root of the spin-spin relaxation time T_2, a reduction of T_2 results in an increase in x_0. As can be observed from the data in Table 2, this parameter x_0 can be used to distinguish the quality of the radiation beam.

Regarding the second result, the values of the homogeneity parameter a are significantly different for proton and electron exposures; in particular, this parameter is greater for dosimeters exposed to protons than for those irradiated with electrons. These different behaviors are strictly correlated with the different LET of the two types of radiation beams. In particular, 19.3 MeV proton beam has an LET of 3.46 keV μm^{-1} in AT, which is more than 10 times the LETs of 7 MeV and 14 MeV electrons, as reported in Table 2. In general, one expects a more diluted and uniform distribution of radicals for low-LET radiation and many regions with high local radical density for high-LET beams. This is because the electrons lose small quantities of energy in each hit and then spread the released energy in large areas of the sample. On the other hand, the energy released by protons for collisional processes is high, and these heavy charged particles lose a great amount of energy near the track. The radicals produced by the two radiation types are distributed into the medium in different ways: a more uniform distribution of free radicals in the samples that gives rise to a extremely diluted spin system with a small spin interaction for electron beams and a distribution characterized by regions with high local radical density that leads to greater radical-radical interaction and correspondingly to a reduction of T_2 for protons. These different situations for different charged particles should be indicated by the EPR line shape becoming more Lorentzian in dosimeters irradiated with high-LET beams (protons) and more Gaussian in dosimeters irradiated with lower-LET beams (electrons). The expected result is that the EPR line shape at increasing LET will become more homogeneously broadened. The value of the homogeneity parameter a for proton beams, which is greater than for electron beams, shows that the EPR line shape is more homogeneous, as reflected by a higher degree of Lorentzian character, than for dosimeters exposed to electrons; i.e., the a parameter increases when the LET of the radiation increases. Therefore, the a value can be used as an indicator of the LET of the radiation.

The increase in the value of a and therefore the tendency of the system to homogeneously broaden more and more with increasing dose (result 3) are correlated with the corresponding increase in the number of free radicals produced. Actually, with increasing dose, the number of radicals per volume unit increases, and therefore an enhancement of the spin-spin interactions occurs. Consequently, when the dose increases, the homogeneity of the EPR line also increases.

From the results for item 4, we can deduce that the spin-lattice relaxation time T_1 [$\propto(x_0^2 \times T_2)^{-1}$] is the same for all the samples exposed to radiation of different LET and that eventual lattice modifications are negligible. This result entails that, even though the beams used have different ionizing abilities and therefore different LET, the interactions of the radical spin with lattice are independent of the beam quality. Presumably, the spin-lattice longitudinal relaxation time T_1 does not change with the quality of the beam.

From this analysis, we conclude that it is possible through a study of microwave power saturation peak-to-peak amplitude to obtain information on the effective LET of the radiation. In fact, using this numerical analysis involving an approximation of the Castner function, we can evaluate the saturation and homogeneity parameters related the distribution of the radicals in the dosimeter.

This study constitutes a useful tool to distinguish radiation quality. When a calibration curve of the values of these parameters is obtained for a great number of dose values and different LET beams, it might be possible through the analysis presented in this paper to measure the effective LET of radiation beams necessary for radiobiological considerations.

ACKNOWLEDGMENTS

The research described in this paper was supported by Gruppo V, INFN, Italy and by the Università di Palermo. The authors are grateful to Dr. Letizia Barone Tonghi at the Radiotherapy Department of the Oncology Hospital ''M.Ascoli'' in Palermo for the electron irradiations and to Dr. Alberto Rovelli at Laboratori Nazionali del Sud in Catania for the proton irradiations and to Ing. Aldo Parlato at Dipartimento di Ingegneria Nucleare in Palermo for the ^{60}Co γ-ray photon irradiations and to Marcello Mirabello for technical support.

Received: February 22, 2006; accepted: June 27, 2006

REFERENCES

1. W. W. Bradshaw, E. W. Crawford, D. G. Cadena and H. A. Spetzler, The use of alanine as a solid state dosimeter. *Radiat. Res.* **17**, 11–21 (1962).
2. D. F. Regulla and U. Deffner, Dosimetry by ESR spectroscopy of alanine. *Int. J. Appl. Radiat. Isot.* **33**, 1101–1114 (1982).
3. H. P. Nette, S. Onori, P. Fattibene, D. Regulla and A. Wieser, Coordinated research efforts for establishing an international radiotherapy dose intercomparison service based on the alanine ESR system. *Appl. Radiat. Isot.* **44**, 7–11 (1993).
4. S. Olsson, S. Bagherian, E. Lund, G. A. Carlsson and A. Lund, Ammonium tartrate as an ESR dosimeter material. *Appl. Radiat. Isot.* **50**, 955–965 (1999).
5. A. Bartolotta, M. Brai, V. Caputo, V. De Caro, L. I. Giannola and G. Teri, ESR solid state dosimetry: Behaviour of various amino acids and blend preparation procedures. *Radiat. Prot. Dosim.* **84**, 293–296 (1999).
6. M. Ikeya, G. M. Hassan, H. Sasaoka, Y. Kinoshita, S. Takaki and C. Yamanaka, Strategy for finding new materials for ESR dosimeters. *Appl. Radiat. Isot.* **52**, 1209–1215 (2000).
7. A. Lund, S. Olsson, M. Bonora, E. Lund and H. Gustafsson, New

materials for ESR dosimetry. *Spectrochim. Acta A* **58**, 1301–1311 (2002).

8. S. Olsson, E. Lund and A. Lund, Development of ammonium tartrate as an ESR dosimeter material for clinical purposes. *Appl. Radiat. Isot.* **52**, 1235–1241 (2000).

9. A. Bartolotta, M. C. D'Oca, M. Brai, V. Caputo, V. De Caro and L. I. Giannola, Response characterization of ammonium tartrate solid state pellets for ESR dosimetry with radiotherapeutic photon and electron beams. *Phys. Med. Biol.* **46**, 461–471 (2001).

10. N. D. Yordanov and V. Gancheva, Properties of ammonium tartrate/ESR dosimeter. *Radiat. Phys. Chem.* **69**, 249–256 (2004).

11. A. Bartolotta, M. Brai, V. De Caro, M. C. D'Oca, L. I. Giannola, A. Kacperek and G. Teri, Response of ammonium tartrate ESR dosimeters to proton clinical beams. *Phys. Med.* **17**, 56–58 (2001).

12. F. Spurný, I. Jadrníčková, V. P. Bamblevski and A. G. Molokanov, Upgrading of LET track-etch spectrometer calibration: Calibration and uncertainty analysis. *Radiat. Meas.* **40**, 343–346 (2005).

13. M. Noll, E. Böck, W. Schöner, P. Egger, C. Wolf, H. Rüdiger and N. Vana, Correlation of the LET-dependent TL-response of LiF:Mg,Ti TL-dosemeters and gentoxic endpoints after proton irradiation. *Appl. Radiat. Isot.* **52**, 1135–1138 (2000).

14. A. Triolo, M. Brai, A. Bartolotta and M. Marrale, Glow curve analysis of TLD-100H irradiated with radiation of different LET: Comparison between two theoretical method. *Nucl. Instrum. Methods A* **560**, 413–417 (2006).

15. A. M. Portis, Electronic structure of F centers. *Phys. Rev.* **91**, 1071–1078 (1953).

16. T. G. Castner, Jr. Saturation of paramagnetic resonance of a V center. *Phys. Rev.* **115**, 1506–1514 (1959).

17. E. Sagstuen, A. Lund, Y. Itagaki and J. Maruani, Weakly coupled proton interactions in the malonic acid radical: Single crystal ENDOR analysis end ESR simulation a microwave saturation. *J. Phys. Chem. A* **104**, 6362–6371 (2000).

18. P. H. G. Sharpe, K. Rajendran and J. P. Sephton, Progress towards an alanine/ESR therapy level reference dosimetry service at NPL. *Appl. Radiat. Isot.* **47**, 1171–1175 (1996).

19. F. J. Ahlers and C. C. J. Schneider, Alanine ESR dosimetry: An assessment of the peak-to-peak evaluation. *Radiat. Prot. Dosim.* **37**, 117–122 (1991).

20. A. Wieser, U. Lettau, U. Fill and D. F. Regulla, The influence of non-radiation induced ESR background signal from paraffin-alanine probes for dosimetry in the radiotherapy dose range. *Appl. Radiat. Isot.* **44**, 59–65 (1993).

21. B. Ciesielski and L. Wielopolski, The effect of dose and radiation quality on the shape and power saturation of ESR signal in alanine. *Radiat. Res.* **140**, 105–111 (1994).

22. E. Malinen, E. Waldeland, E. O. Hole and E. Sagstuen, LET effects following neutron irradiation of lithium formate EPR dosimeters. *Spectrochim. Acta A* **63**, 861–869 (2006).